



This is the accepted manuscript made available via CHORUS. The article has been published as:

# Suppression of Beneficial Mutations in Dynamic Microbial Populations

Philip Bittihn, Jeff Hasty, and Lev S. Tsimring

Phys. Rev. Lett. **118**, 028102 — Published 12 January 2017

DOI: [10.1103/PhysRevLett.118.028102](https://doi.org/10.1103/PhysRevLett.118.028102)

# Suppression of beneficial mutations in dynamic microbial populations

Philip Bittihn,<sup>1,\*</sup> Jeff Hasty,<sup>1,2,3,†</sup> and Lev S. Tsimring<sup>1,†</sup>

<sup>1</sup>*BioCircuits Institute, University of California San Diego, La Jolla, California 92093, USA*

<sup>2</sup>*Department of Bioengineering, University of California San Diego, La Jolla, California 92093, USA*

<sup>3</sup>*Molecular Biology Section, Division of Biological Science, University of California San Diego, La Jolla, California 92093, USA*

(Dated: October 6, 2016)

Quantitative predictions for the spread of mutations in bacterial populations are essential to interpret evolution experiments and to improve the stability of synthetic gene circuits. We derive analytical expressions for the suppression factor for beneficial mutations in populations that undergo periodic dilutions, covering arbitrary population sizes, dilution factors and growth advantages in a single stochastic model. We find that the suppression factor grows with the dilution factor and depends non-trivially on the growth advantage, resulting in the preferential elimination of mutations with certain growth advantages. We confirm our results by extensive numerical simulations.

The fixation of random mutations is the driving force of evolutionary adaptation. Mutations can also be problematic, e.g., in synthetic biology, where long-term stability is required to reliably and safely translate more than a decade of circuit design to in-vivo or industrial settings, but disabling a synthetic gene network is often beneficial to the cell [1]. Maintaining a bacterial strain over long times in a lab setting to study its evolution [2, 3] requires enforcing certain population dynamics. To be able to interpret the results and build quantitative models, it is therefore essential to understand how these dynamics themselves alter the impact of beneficial mutations.

We consider the most widely-used protocol, serial passage [3], which is characterized by phases of exponential growth alternating with strong reductions in population size (“bottlenecks”). A constant population size maintained, e.g., in a turbidostat [4] or in microfluidic traps [5] serves as the reference scenario for which theoretical results are well-known [6–9]. These established results were recently extended to include populations that vary in size [10, 11], transmission phases [12] or clonal interference [13]. While repeated pruning of an exponentially growing population was considered before [14–17], closed-form predictions currently only exist for certain limiting cases and, as we show below, their range of applicability is even more limited than previously thought. Therefore, a complete and consistent picture of the fixation process during serial passage is still lacking. Using two complementary approaches for a single evolutionary model, we derive closed-form analytical expressions which provide a quantitative characterization of mutant fixation for arbitrary dilution factors, population sizes and selective advantages that agrees with direct numerical simulations. We use a stochastic model of division by binary fission:

$$X \xrightarrow{\alpha(1-\mu)} 2X; \quad X \xrightarrow{\alpha\mu} X + Y; \quad Y \xrightarrow{(1+s)\alpha} 2Y \quad (1)$$

$X$  and  $Y$  represent wild-type and mutant cells, respectively. To obtain analytical results, memoryless reactions are assumed, resulting in exponentially distributed division times. However, we will later extend some of our results to more realistic distributions. In Eq. (1),

$\alpha$  is the wild-type division rate,  $\mu \leq 1$  is the mutation probability upon division,  $s \geq 0$  is the growth rate change of the mutant. For a *constant* population with  $N_c$  individuals, a random individual is removed after each division (Moran process). In *dynamic* populations, cells divide freely for some time  $T$ , then the population is pruned (“diluted”) to a fixed number of survivors  $N_s$  and the cycle repeats. The latter resembles subculturing in fresh growth medium in the serial passage protocol. The survival probability is assumed to be equal for all cells. On average, the population size before dilution is  $fN_s$ , where  $f = \exp(\alpha T)$  is the dilution factor. We use  $N_c = N_s(f - 1)/\log(f)$ , rounded to the nearest integer, to achieve approximately the same time-averaged population size in both cases (for  $\mu = 0$ ).

Typical trajectories of the model are depicted in Fig. 1a and b. The fixation time  $\tau$  is defined as the time until the population consists of only mutants. We numerically computed the average fixation times  $\tau_c$  and  $\tau_d$  for a constant population and the dynamic protocol, respectively (see Fig. 1c). Figure 1d shows that  $\tau_d > \tau_c$  across all  $s$ , meaning that the dynamic population can withstand the evolutionary pressure of beneficial mutations longer. Below, we will calculate the fixation probability  $p$  of a single mutation under the influence of the above population dynamics. If  $\mu$  is sufficiently small, there is a direct correspondence between  $\tau$  and  $p$ : Based on the idea of the slow-scale stochastic simulation algorithm [19], the mutation rate can be approximated by  $\alpha\mu\bar{n}_X$  [20], where  $\bar{n}_X$  is the time-averaged number of wild-type cells for  $\mu = 0$ . Since only a fraction  $p$  of mutations becomes fixed eventually, the average fixation time is  $\tau = (\alpha\mu\bar{n}_X p)^{-1}$ , implying  $\tau_d/\tau_c = p_c/p_d$ .

We will first use a diffusion approach to characterize  $p$  for  $s$  close to zero and then employ a recently developed branching process approach for larger  $s$ .

*Diffusion approximation.* This approach was initially developed by Kimura [9] and is valid for weakly beneficial mutations when the fixation process is dominated by genetic drift. In contrast to Wahl *et al.* [14, 15], we

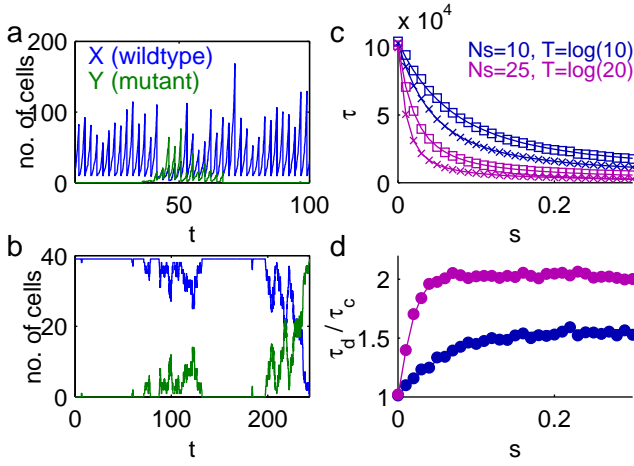


FIG. 1. Typical trajectories of the model (1) for **(a)** a dynamic population undergoing repeated pruning and **(b)** a constant population. Parameters:  $\alpha = 1$ ,  $N_s = 10$ ,  $T = \log(10)$ ,  $\mu = 10^{-3}$ , resulting in  $f = 10$ ,  $N_c = 39$ . **(c)** Fixation times in constant and dynamic populations from 10000 stochastic simulations using an accelerated algorithm [18]. **(d)** Fixation time ratio. Solid lines in (c) and (d) indicate exact numerical values from Markov models for a constant population and a population pruned when reaching a fixed size  $fN_s$ .

will consider all contributions to stochastic fluctuations, including cell division, and model random selection upon dilution with the exact hypergeometric distribution. Let  $M_{\delta y}(y)$  and  $V_{\delta y}(y)$  be the mean and variance, respectively, of the change of the fraction of mutants from the current generation to the next, given that the current fraction of mutants is  $y = n_Y/(n_X + n_Y)$ . Then, with the definition  $G(y) = \exp(-2 \int_0^y M_{\delta y}(y')/V_{\delta y}(y') dy')$ , the probability of fixation  $u(y)$  is given by  $u(y) = \int_0^y G(y') dy' / \int_0^1 G(y') dy'$ . Let  $\Lambda$  be the Taylor expansion of  $M_{\delta y}(y)/V_{\delta y}(y)$  near  $s = 0$  up to the order of  $s$  chosen such that  $\Lambda$  is independent of  $y$ . Then, the fixation probability for an initial fraction of mutants  $y$  is

$$u(y) = \frac{1 - \exp(-2\Lambda y)}{1 - \exp(-2\Lambda)}. \quad (2)$$

For dynamic populations, we define  $y$  as the fraction of mutants at the beginning of each cycle. Therefore,  $M_{\delta y}(y)/V_{\delta y}(y)$  describes the effect of one growth cycle and subsequent pruning. Mutations occur at any time during the growth phase, implying that the initial fraction of mutants  $y$  for Eq. (2) (i.e., at the beginning of the cycle following the mutation's introduction) is a random variable. We accommodate this by approximating  $p_d \approx u_d(\bar{y}_d)$ , where  $\bar{y}_d$  is the average initial fraction of mutants. Hence, estimating  $p_d$  amounts to calculating  $\Lambda_d$  and  $\bar{y}_d$ .

To obtain  $M_{\delta y}(y)/V_{\delta y}(y)$  for dynamic populations and subsequently  $\Lambda_d$ , we note that, for the growth phase, the wild-type and mutant subpopulations are described by

simple birth processes which start with  $(1 - y_0)N_s$  and  $y_0N_s$  individuals, respectively. At the end of a cycle,  $t = T$ , the mean and variance for a population starting with  $N_0$  individuals and a division rate  $\lambda$  are:

$$M_\lambda(N_0) = N_0 \exp(\lambda T) \quad (3a)$$

$$V_\lambda(N_0) = \xi^2 N_0 \exp(\lambda T) [\exp(\lambda T) - 1]. \quad (3b)$$

$\xi^2$  will allow us later to scale the stochastic fluctuations during growth, but we will initially evaluate only the case  $\xi^2 = 1$ , which corresponds to the model (1).

As dilution does not, on average, alter the fraction of mutants, Eq. (3) can be used directly to obtain  $M_{\delta y}$ , whereas for  $V_{\delta y}$ , Eq. (3) is combined with the variance of the hypergeometric distribution for the dilution event [20]. A first-order expansion of  $M_{\delta y}/V_{\delta y}$  around  $s = 0$  then leads to  $\Lambda_d \approx 2s(N_s - \xi^2)f \log(f)/[(f-1)(1 + \xi^2)]$ . To estimate  $\bar{y}_d$ , we consider a mutant subpopulation that first appears at time  $\theta$  into a cycle and initially consists of  $m_s$  individuals. For the model (1)  $m_s = 1$ , since the second reaction produces a single mutant cell. By the end of the initial cycle, the mutant subpopulation will have grown for a time  $T - \theta$  to a size larger than  $m_s$ . As might be intuitive (and can be shown explicitly [20]), the probability distribution of  $\theta$  is  $p_{\text{mut}}(\theta) = \exp(\alpha\theta)/\int_0^T \exp(\alpha\theta') d\theta'$ , i.e. proportional to the average rate of division events at a given time  $\theta$  within a cycle. Using  $p_{\text{mut}}(\theta)$ , we obtain the average sizes of the wild-type and mutant subpopulations for random  $\theta$  as weighted averages of Eq. (3a) and estimate the average initial fraction of mutants as  $\lim_{N_s \rightarrow \infty} N_s \bar{y}_d = \frac{m_s(f^s - 1)}{s(f-1)}$ , independent of  $\xi^2$  [20].

Substituting  $\bar{y}_d$  and  $\Lambda_d$  into Eq. (2), we obtain

$$p_d = \frac{1 - \exp\left(-\frac{2m_s}{1+\xi^2} \frac{(N_s - \xi^2)f \log(f)(f^s - 1)}{N_s(f-1)^2}\right)}{1 - \exp\left(-\frac{2}{1+\xi^2} \frac{(N_s - \xi^2)f \log(f)}{f-1} s\right)}. \quad (4)$$

Formula (4) can also be used for the constant population case by replacing  $N_s \rightarrow N_c$  and taking the limit  $f \rightarrow 1$ , so it reduces to

$$p_c = \frac{1 - \exp(-2m_s s/(1 + \xi^2))}{1 - \exp(-2N_c s/(1 + \xi^2))}. \quad (5)$$

Note that a more accurate approximation of  $p_c$  can be obtained by calculating  $\Lambda_c$  directly [20]. For  $\xi^2 = 1$  and  $m_s = 1$ , the theoretical estimates (4), (5) are plotted in Fig. 2a. As expected, the theory matches the numerical data towards  $s = 0$ . The accuracy is remarkable considering it being a continuous approximation of a discrete process in small populations and the usage of a large- $N_s$  approximation for  $\bar{y}_d$ . A Taylor expansion of  $\tau_d/\tau_c = p_c/p_d$  around  $s = 0$  yields (for large  $N_s$ )

$$\tau_d/\tau_c \approx 1 + sN_s \frac{(f-1)[1 - \Delta^{-1}(f)]}{(1 + \xi^2) \log(f)} + \mathcal{O}(s^2) \quad (6)$$

with  $\Delta(f) = [(f-1)/\log f]^2/f$ . For any  $f > 1$ ,  $\Delta$  is larger than 1, so the slope of  $\tau_d/\tau_c$  at  $s = 0$  is positive. Thus, periodic dilutions do not impact neutral mutations

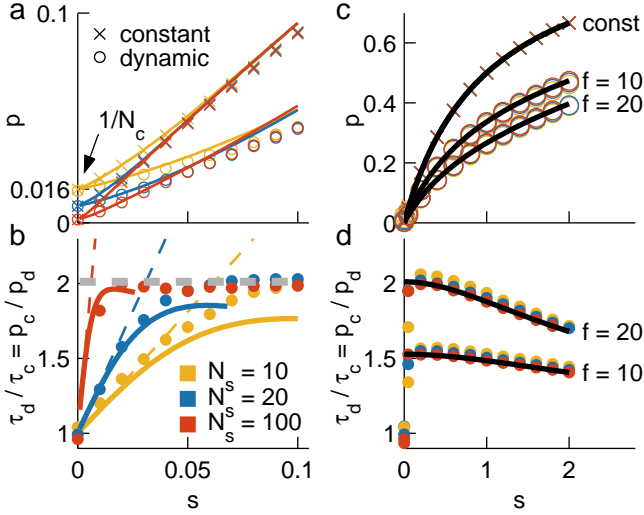


FIG. 2. **(a)** Fixation probabilities from numerical simulations (symbols) compared to diffusion approximation, Eqs. (5), (4) (lines). **(b)** Numerical  $\tau_d/\tau_c$  (symbols) and diffusion approximation (lines). Colored dashed lines: initial slope at  $s = 0$  according to Eq. (6); gray dashed line: asymptotic ratio  $\Delta$ , Eq. (7). For all data in (a) and (b)  $f = 20$ ,  $\xi^2 = 1$ ,  $m_s = 1$ . **(c), (d)** Numerical  $p$  and  $\tau_d/\tau_c$  (symbols) compared to branching process approximation, Eqs. (9), (11) (lines). The  $y$  intercept in (d) is also  $\Delta$ .

as expected, while beneficial mutations are suppressed by a factor that grows with  $s$  in the vicinity of  $s = 0$ . The slope of  $\tau_d/\tau_c$  increases with  $N_s$ , in agreement with Fig. 2b.

First taking the limit  $N_s \rightarrow \infty$  and subsequently considering small  $s$ , we obtain  $p_d \approx \frac{2m_s}{1+\xi^2} \Delta^{-1} s$  and  $p_c \approx \frac{2m_s}{1+\xi^2} s$  from Eqs. (4) and (5), respectively, which corresponds to the only limit for which analytical results were previously available [15]. The factor by which mutations are suppressed by serial dilutions in this limit is therefore

$$\lim_{s \rightarrow 0} \lim_{N_s \rightarrow \infty} \frac{\tau_d}{\tau_c} = \Delta(f), \quad (7)$$

which is shown as a gray dashed line in Fig. 2b. For any finite population size, there is a smooth transition of  $\tau_d/\tau_c$  towards  $\Delta$  with the rate indicated by Eq. (6).

*Branching process approximation.* As a complementary approach, we employ the framework developed by Uecker & Hermisson [21]. Based on an inhomogeneous branching processes, they derived the following expression for the fixation probability:

$$p = 2 \left[ 1 + \int_0^\infty (\lambda + \delta)(t) \exp \left( - \int_0^t (\lambda - \delta)(t') dt' \right) dt \right]^{-1}, \quad (8)$$

where  $\lambda(t)$  and  $\delta(t)$  are the per capita birth and death rates, respectively, of the mutant subpopulation in the “branching limit”. It implicitly assumes that stochastic fluctuations of the wildtype population size can be ig-

nored and thus we do not expect this approximation to capture finite population size effects present for small  $s$ . For a constant population, we have the per capita birth rate  $\lambda_c(t) = (1 + s)\alpha$  for the mutant subpopulation. Mutant individuals are replaced by wild-type individuals when a wild-type individual is born with rate  $\alpha n_X$  and a mutant is chosen for removal with probability  $\frac{n_Y}{n_X + n_Y + 1} \approx \frac{n_Y}{n_X}$ . The per capita death rate is therefore  $\delta_c(t) = \alpha$ . Substitution into Eq. (8) yields

$$p_c = \frac{s}{1 + s}. \quad (9)$$

For the population undergoing serial dilutions, we assume small time intervals of length  $\sigma \ll T$  during which cells die with rate  $\sigma^{-1} \log f$ , reducing the population size from  $fN_s$  to  $N_s$  exactly in the branching limit. Assuming the mutation is introduced at time  $\theta$  into a cycle, these “windows of death” occur at times  $t_i = iT - \theta$ ,  $i = 1, 2, \dots$ . Therefore, we have

$$\lambda_d(t) = (1 + s)\alpha \quad (10a)$$

$$\delta_d(t) = \begin{cases} \frac{\log f}{\sigma} & \exists i \in 1, 2, \dots, t_i < t < t_i + \sigma \\ 0 & \text{otherwise} \end{cases}. \quad (10b)$$

Substituting these rates into Eq. (8) and taking the limit  $\sigma \rightarrow 0$  yields the fixation probability  $p_d(\theta)$  conditioned on the time of appearance,  $\theta$  [20]. By averaging over  $p_{\text{mut}}(\theta)$ , we obtain the unconditional fixation probability

$$p_d = \frac{1}{f-1} \left[ f F \left( \frac{f-1}{1-f-s} \right) - F \left( \frac{f-1}{f^{1+s}-f} \right) \right], \quad (11)$$

where  $F(\cdot)$  is defined using the hypergeometric function  ${}_2F_1(a, b; c; z)$  as  $F(x) = {}_2F_1(1, 1/(1+s); 1+1/(1+s); -x)$ . Figures 2c,d show a comparison of this theory with numerical simulations. As  $s \rightarrow 0$ ,  $p_d$  converges to 0, but  $\tau_d/\tau_c = p_c/p_d$  approaches the finite value  $\Delta$ , which is identical to the result derived earlier from the diffusion approach, Eq. (7), and therefore consistent with the implicit assumption of large populations. In contrast, for finite population sizes, only the diffusion approximation correctly captures the immediate vicinity of  $s = 0$  where  $\tau_d/\tau_c \rightarrow 1$  (compare Figures 2b and d).

Exponential division time distributions, which have zero mode, are unrealistic, because cells need time to mature before the next division. In reality, the division time distribution has a clear peak with a Fano factor smaller than 1 [22]. According to Eqs. (6) and (7), the initial increase of  $\tau_d/\tau_c$  should be faster for a less stochastic division process (i.e. smaller  $\xi^2$ ), while the plateau value  $\Delta$  should not depend on  $\xi^2$ .

To test these predictions, we consider an extension of Eq. (1), where the simple memoryless division is replaced by a process with  $k$  stages, which has been characterized in detail by Kendall [23]: The total division time  $d$  of, e.g., a wild-type cell is distributed according to  $2kad \sim \mathcal{X}_{2k}^2$ . After individuals have established an

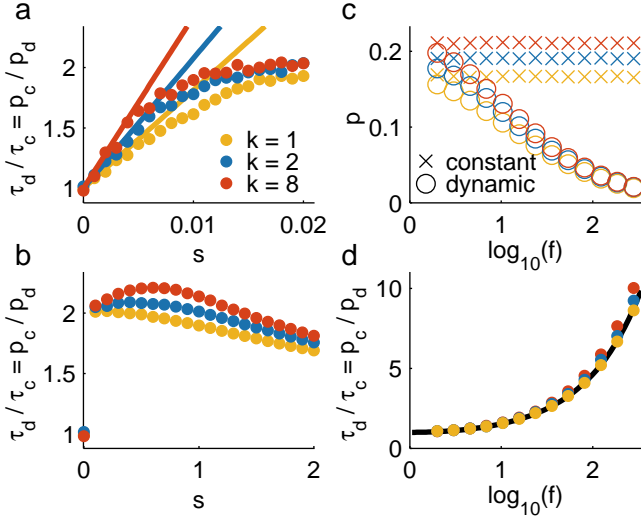


FIG. 3. Fixation probabilities and ratios in the multi-stage model. (a)  $\tau_d/\tau_c$  for small  $s$  for different  $k$  in numerical simulations (symbols). Lines indicate the slope predicted by Eq. (6) with  $\xi^2 = \frac{2\log(2)^2}{k}$ . (b)  $\tau_d/\tau_c$  from numerical simulations for larger  $s$ . (c)  $p_c$  and  $p_d$  as functions of the dilution factor  $f$ . (d)  $\tau_d/\tau_c$  for the data shown in (c) compared to the analytical approximation, Eq. (7). Parameters:  $N_s = 50$ ,  $f = 20$  (a,b) and  $N_s = 20$ ,  $s = 0.2$  (c,d).

equilibrium distribution across the  $k$  different stages, the population grows like  $\exp(\alpha k(2^{1/k} - 1)t)$ , leading to deterministic growth  $\propto 2^{\alpha t}$  as  $k \rightarrow \infty$ . We use an adjusted growth rate of  $\alpha[k(2^{1/k} - 1)]^{-1}$  in numerical simulations to maintain an effective population growth according to  $\exp(\alpha t)$ , resulting in the same average population size for unchanged cycle lengths  $T$ . For a population of individuals starting in the first stage, the initial population growth is delayed, reducing the effective initial size of the mutant subpopulation from 1 to  $m_s = 1/[2k(1 - 2^{-1/k})]$ . The variance of the population size is different from that of a memoryless division process by a factor of  $\xi^2 \approx \frac{2\log(2)^2}{k}$ .

Figure 3a shows numerical simulations for different  $k$ , along with the approximation of Eq. (6), substituting the changed value for  $\xi^2$ . Note that this neglects the fact that division events in the mutant subpopulation are initially correlated. Nevertheless, there is good quantitative agreement with Eq. (6). Figure 3b shows that there are some quantitative differences for larger  $s$ , but, according to Fig. 3d, for small  $s$  beyond the initial region of increase for finite population sizes (cf. Fig. 2b),  $\tau_d/\tau_c$  is indeed at most weakly dependent on  $k$ , as predicted by Eq. (7).

In this study, we have developed a complete analytical characterization of the fixation probability of beneficial mutations in exponentially growing populations with re-

peated bottlenecks, akin to serial passage. The most intriguing result is that the impact of serial passage on the fixation probability depends non-trivially on the growth rate change  $s$ , a novel effect not seen in the previously considered large-population, low- $s$  limit, where all fixation probabilities were found to be proportional to  $s$  and therefore the ratio  $p_c/p_d$  is a constant [15, 17]. Therefore, the experimental protocol acts as a filter which biases the distribution of selective advantages of fixed mutations with respect to a constant population or serial passage with different  $f$ . Our results provide quantitative predictions for three distinct regimes: Firstly, starting from  $p_c/p_d = 1$  at  $s = 0$  (no suppression of neutral mutations), the suppression factor increases gradually (and more quickly for larger  $N_s$ ) as  $s$  increases, which is captured by the diffusion approach, Eqs. (4), (5), (6). Secondly, in an intermediate regime,  $p_c/p_d$  reaches a plateau value  $\Delta$ , Eq. (7), which only depends on the dilution factor  $f$ . Thirdly, towards large  $s$ , the fixation probability for the serial passage protocol slowly returns to that for a constant population, as described by the branching process approximation, Eq. (11).

To our knowledge, no previous analytical results existed for the first and third regime. For the plateau, we find  $\Delta$  to be monotonic with respect to  $f$  (cf. Fig. 3d) and to approach 1 for  $f \rightarrow 1$ , which is in contrast to the prediction of an optimal dilution factor  $f$  from the previously derived formula  $\Delta' = f/(\log f)^2$  [15]. However, this earlier result used a binomial distribution for the dilution process, which is only a good approximation for large  $f$  [20], and indeed, in this regime,  $\Delta' \approx \Delta$ . Our prediction is not only confirmed by full numerical simulations, but also intuitive as frequent but mild dilutions are experimentally indistinguishable from a constant population. Furthermore, as can be shown explicitly [20], it is consistent with Ref. [17].

Equation (6) reaches  $\Delta$  at a selective advantage  $\delta s = \frac{(f-1)(1+\xi^2)}{fN_s \log(f)}$ , providing an order-of-magnitude estimate for regimes of validity of Eq. (6) ( $s \lesssim \delta s$ ) vs. Eq. (11) ( $s \gtrsim \delta s$ ), which is particularly important for very small population sizes, when  $\delta s$  is large. For larger populations, the value of  $s$  at which  $\Delta$  is attained is negligible compared to the region in which  $\tau_d/\tau_c \approx \Delta$  (cf. Fig. 2b,  $N_s = 100$ ), which indicates equal suppression of mutations conferring arbitrary moderate growth rate changes. While, in reality, cell division and mutation are far more complex than described by the model (1), our results establish a baseline that can be used to gauge the influence of other effects. We confirmed that they hold qualitatively for more realistic division statistics and even quantitatively through the proxy parameters  $\xi^2$  and  $m_s$  in the low- $s$  regime (cf. Fig. 3). Generalizing the branching process approximation to take these statistics into account for larger  $s$  presents an interesting direction of future research. We also found that the exact periodicity of di-

lutions is not essential, as pruning at a fixed number of cells  $fN_s$  leads to almost identical numerical results [20]. Another possible extension is to consider non-exponential growth, although a previous study found little effect for the specific case considered there [15].

Our quantitative analytical results provide a framework for the interpretation of evolution experiments involving serial passage by predicting how the experimental protocol itself can facilitate or suppress the fixation of mutations with certain selective advantages, which is a prerequisite for investigating the relation between population level adaptation and its molecular basis for other than neutral mutations [24]. They may also provide guidance for limiting the impact of undesired mutations in engineered bacteria by adjusting the experimental protocol or employing synthetic ecologies to shape their inherent population dynamics.

P.B. acknowledges support from HFSP fellowship LT000840/2014-C, J.H. acknowledges support from NIH grant R01-GM069811, and L.T. acknowledges support from ONR grant N00014-16-1-2093 and NSF grant MCB-1121748. Authors also acknowledge partial support from the San Diego Center for Systems Biology, NIH grant P50-GM085764.

---

\* pbittihn@ucsd.edu

† Co-senior authors

- [1] S. C. Sleight, B. A. Bartley, J. A. Lieviant, and H. M. Sauro, *Journal of biological engineering* **4**, 12 (2010).
- [2] E. Loh, J. J. Salk, and L. A. Loeb, *Proceedings of the National Academy of Sciences of the United States of America* **107**, 1154 (2010).
- [3] M. J. Wiser, N. Ribbeck, and R. E. Lenski, *Science* **342**, 1364 (2013).
- [4] T. G. Watson, *Journal of Applied Chemistry and Biotechnology* **22**, 229 (2007).
- [5] A. Prindle, P. Samayoa, I. Razinkov, T. Danino, L. S. Tsimring, and J. Hasty, *Nature* **481**, 39 (2012).
- [6] R. A. Fisher, *Proceedings of the Royal Society of Edinburgh* **50**, 205 (1930).
- [7] R. A. Fisher, *Proceedings of the Royal Society of Edinburgh* **42**, 321 (1922).
- [8] J. Haldane, *Mathematical Proceedings of the Cambridge Philosophical Society* **23**, 838 (1927).
- [9] M. Kimura, *Genetics* **47**, 713 (1962).
- [10] S. P. Otto and M. C. Whitlock, *Genetics* **146**, 723 (1997).
- [11] E. Pollak, *Theoretical Population Biology* **57**, 51 (2000).
- [12] A. Handel and M. R. Bennett, *Genetics* **180**, 2193 (2008).
- [13] P. R. A. Campos and L. M. Wahl, *Evolution* **63**, 950 (2009).
- [14] L. M. Wahl and P. J. Gerrish, *Evolution* **55**, 2606 (2001).
- [15] L. M. Wahl, P. J. Gerrish, and I. Saika-Voivod, *Genetics* **162**, 961 (2002).
- [16] J. M. Heffernan and L. M. Wahl, *Theoretical Population Biology* **62**, 349 (2002).
- [17] J. E. Hubbarde and L. M. Wahl, *Mathematical Biosciences* **213**, 113 (2008).
- [18] W. H. Mather, J. Hasty, and L. S. Tsimring, *Bioinformatics* **28**, 1230 (2012).
- [19] Y. Cao, D. T. Gillespie, and L. R. Petzold, *The Journal of chemical physics* **122**, 14116 (2005).
- [20] See Supplemental Material at ...link... for a detailed derivation..
- [21] H. Uecker and J. Hermisson, *Genetics* **188**, 915 (2011).
- [22] S. Iyer-Biswas, C. S. Wright, J. T. Henry, K. Lo, S. Burov, Y. Lin, G. E. Crooks, S. Crosson, A. R. Dinner, and N. F. Scherer, *Proceedings of the National Academy of Sciences of the United States of America* **111**, 15912 (2014).
- [23] D. G. Kendall, *Biometrika* **35**, 316 (1948).
- [24] S. Wielgoss, J. E. Barrick, O. Tenaillon, S. Cruveiller, B. Chane-Woon-Ming, C. Médigue, R. E. Lenski, and D. Schneider, *G3 (Bethesda, Md.)* **1**, 183 (2011).